

# Adiabatic quantum dynamics of a random Ising chain across its quantum critical point

Tommaso Caneva

*International School for Advanced Studies (SISSA), Via Beirut 2-4, I-34014 Trieste, Italy*

Rosario Fazio

*International School for Advanced Studies (SISSA), Via Beirut 2-4, I-34014 Trieste, Italy and  
NEST-CNR-INFM & Scuola Normale Superiore di Pisa, Piazza dei Cavalieri 7, 56126 Pisa, Italy*

Giuseppe E. Santoro

*International School for Advanced Studies (SISSA), Via Beirut 2-4, I-34014 Trieste, Italy  
CNR-INFM Democritos National Simulation Center, Via Beirut 2-4, I-34014 Trieste, Italy and  
International Centre for Theoretical Physics (ICTP), P.O.Box 586, I-34014 Trieste, Italy*

(Dated: October 29, 2018)

We present here our study of the adiabatic quantum dynamics of a random Ising chain across its quantum critical point. The model investigated is an Ising chain in a transverse field with disorder present both in the exchange coupling and in the transverse field. The transverse field term is proportional to a function  $\Gamma(t)$  which, as in the Kibble-Zurek mechanism, is linearly reduced to zero in time with a rate  $\tau^{-1}$ ,  $\Gamma(t) = -t/\tau$ , starting at  $t = -\infty$  from the quantum disordered phase ( $\Gamma = \infty$ ) and ending at  $t = 0$  in the classical ferromagnetic phase ( $\Gamma = 0$ ). We first analyze the distribution of the gaps, occurring at the critical point  $\Gamma_c = 1$ , which are relevant for breaking the adiabaticity of the dynamics. We then present extensive numerical simulations for the residual energy  $E_{\text{res}}$  and density of defects  $\rho_k$  at the end of the annealing, as a function of the annealing inverse rate  $\tau$ . Both the average  $E_{\text{res}}(\tau)$  and  $\rho_k(\tau)$  are found to behave logarithmically for large  $\tau$ , but with different exponents,  $[E_{\text{res}}(\tau)/L]_{\text{av}} \sim 1/\ln^\zeta(\tau)$  with  $\zeta \approx 3.4$ , and  $[\rho_k(\tau)]_{\text{av}} \sim 1/\ln^2(\tau)$ . We propose a mechanism for  $1/\ln^2 \tau$ -behavior of  $[\rho_k]_{\text{av}}$  based on the Landau-Zener tunneling theory and on a Fisher's type real-space renormalization group analysis of the relevant gaps. The model proposed shows therefore a paradigmatic example of how an adiabatic quantum computation can become very slow when disorder is at play, even in absence of any source of frustration.

PACS numbers:

## I. INTRODUCTION

How effective is it to execute a given computational task by slowly varying in time the Hamiltonian of a quantum system? Is it possible to find the ground state of a classical system by slowly annealing away its quantum fluctuations? What is the density of defects left over after a passage through a continuous (quantum) phase transition? These seemingly different problems, rubricated under the names of Adiabatic quantum computation<sup>1</sup>, Quantum Annealing<sup>2,3,4,5,6,7</sup> and Kibble-Zurek topological defect formation in quantum phase transitions<sup>8</sup>, are ultimately related to the understanding of the failure of the adiabatic approximation in a many-body system passing through a quantum critical point.

Adiabatic quantum computation (AQC), *alias* Quantum Annealing (QA), is a possible alternative to the standard circuit-theory approach to Quantum Computation (QC)<sup>9</sup>. Indeed, as shown by Aharonov *et al.*<sup>10,11</sup>, any quantum algorithm can be equivalently reformulated in terms of the adiabatic evolution of an appropriate time-dependent Hamiltonian  $H(t) = [1 - f(t)]H_{\text{in}} + f(t)H_{\text{fin}}$ ,  $f(t)$  being a generic function of time such that  $f(0) = 0$  and  $f(t_{\text{fin}}) = 1$ . The initial Hamiltonian  $H_{\text{in}}$ , for which we know the ground state, provides the input of the algorithm. The final Hamiltonian  $H_{\text{fin}}$  is constructed appropriately so as to possess the solution of the computational

task as its ground state. The knowledge of the equivalence of computational power between the two different QC schemes, however, does not provide a practical way of constructing  $H_{\text{in}}$  and  $H_{\text{fin}}$  for a given computational problem. Understanding what computational problems can be efficiently solved by AQC-QA is, in general, a very difficult problem. In order to solve the task one has to find a suitable path in Hamiltonian space in such a way that the resulting Schrödinger evolution efficiently drives the system from some simple initial quantum state  $|\Psi_{\text{in}}\rangle$  to the sought final ground state<sup>12,13</sup>. The accuracy of the computation, which relies on the possibility for the system to remain in the instantaneous ground state during the dynamics, is ultimately limited by the fact that at specific times the instantaneous Hamiltonian presents a gap between the ground and the first excited state which closes on increasing the size of the input.

On totally independent grounds, the study of topological defect formation goes back to the 80's, motivated by the effort to understand signatures of phase transitions which have occurred in the early universe<sup>14,15</sup> by determining the density of defects left in the broken symmetry phase as a function of the rate of quench. By means of the so called Kibble-Zurek mechanism, a scaling law relates the density of defects to the rate of quench. The suggestion of Zurek to simulate transitions in the early universe by means of condensed matter system has stimulated an

intense experimental activity<sup>16,17</sup> aimed at verifying the Kibble-Zurek theory. The understanding of defect formation was later explored also in the case of a quantum phase transition<sup>8,18</sup>, where the crossing of the critical point is done by varying a parameter in the Hamiltonian. These works have stimulated an intense activity where several different quantum systems undergoing a quantum phase transition were scrutinized. In the past couple of years there have been a number of results obtained in the area of adiabatic dynamics of many-body systems<sup>19,20</sup>. Most of the works concentrated on the one-dimensional Ising model. Soon after the appearance of Ref. 8, Dziarmaga<sup>21</sup> obtained analytically the scaling law for the density of defects by resorting to the exact solution of Pfeuty<sup>22</sup>. A detailed analysis *a' la Landau-Zener* was presented in Refs.<sup>23,24,25</sup>. The effect of an external noise on the adiabatic evolution and its consequences for the Kibble-Zurek mechanism has been discussed in<sup>26</sup>. Recently, quenches in Bose-Hubbard models were analyzed<sup>27,28</sup> as well. Observables which were analyzed to quantify the loss of adiabaticity in the critical region were typically the density of defects left behind in the broken symmetry phase, the fidelity of the evolved state with respect to the ground state, and, in few cases, also the residual block entropy<sup>29,30</sup>. This brief overview of recent works accounts only for papers dealing with adiabatic dynamics, without touching the vast literature treating the case of sudden quenches.

In the present work we analyze the adiabatic dynamics in a one-dimensional quantum disordered Ising model in a random transverse field. The reasons for considering this problem are various. First of all it is an important ground test for the Kibble-Zurek mechanism. In addition, although in a very simplified manner, it may help in understanding more interesting problems that can be formulated in terms of interacting Ising spins, Traveling Salesman<sup>31</sup> and Satisfiability<sup>32</sup> problems being only two well-known examples. The simplicity of our test problem lies in the particularly simple geometry of the interactions, which forbids frustration. The only ingredient that our problem shares with more challenging computational tasks is the fact that the interactions are chosen to be random. This feature, the presence of disorder, makes the problem interesting and non-trivial for a physically inspired computational approach based on AQC-QA.

Of particular relevance for us is Ref.33 where this model was analyzed first, and the anomalously slow dynamics characterized by an average density of kinks which vanishes only logarithmically with the annealing rate. Here we extend this work by presenting a detailed analysis of the statistics of both the residual energy and kink density. In a disordered chain, the formation of the kinks is no longer translational invariant and therefore it affects in a non-trivial way, as we will show below, the scaling of the residual energy.

The rest of the paper is organized as follows: In Sec. II we define the problem and the technique to solve the adiabatic dynamics of the random Ising chain, and next, in

Sec. III, we introduce the quantities — residual energy and density of defects — that we calculate to quantify the departure from the adiabatic ground state. In Sec. IV we present our numerical results for both these quantities, together with an analysis of the large-annealing-time behavior of the density of defects, based on the Landau-Zener theory, explicitly showing the slow dynamics which the disorder entails. In the final section we present a critical assessment of our findings, and a concluding discussion.

## II. THE MODEL

As discussed in the Introduction, our aim is to analyze the adiabatic dynamics of a one-dimensional random Ising model defined by the Hamiltonian

$$H(t) = - \sum_i J_i \sigma_i^z \sigma_{i+1}^z - \Gamma(t) \sum_i h_i \sigma_i^x . \quad (1)$$

In the previous expression  $\sigma_i^\alpha$  ( $\alpha = x, z$ ) are Pauli matrices for the  $i$ -th spin of the chain,  $J_i$  are random couplings between neighboring spins, and  $h_i$  are random transverse fields. The time-dependent function  $\Gamma(t)$  rescaling the transverse field term allows us to drive the system from a region of infinitely high transverse fields ( $\Gamma = \infty$ , where the ground state has all spins aligned along  $x$ , see below), to the case of a classical Ising model ( $\Gamma = 0$ ). Specifically, we will take in the following  $\Gamma(t)$  to be a linear function of time characterized by an annealing rate  $\tau^{-1}$

$$\Gamma(t) = -\frac{t}{\tau} \quad \text{for } t \in (-\infty, 0] .$$

In one-dimension, and for nearest-neighbor couplings, there is no frustration associated to the random nature of the couplings  $J_i$ : by appropriately performing spin rotations of  $\pi$  along the  $x$ -spin axis, we can always change the desired  $\sigma_i^z$  into  $-\sigma_i^z$  and invert accordingly the signs of the couplings in such a way that all  $J_i$ 's turn out to be non-negative. We therefore assume that the  $J_i$  are randomly distributed in the interval  $[0, 1]$ , specifically with a flat distribution  $\pi[J] = \theta(J)\theta(1 - J)$ , where  $\theta$  is the Heaviside function. The same distribution is used for the random field  $\pi[h] = \theta(h)\theta(1 - h)$ . This is different from the model considered in Ref.33, where the disorder was introduced in the exchange coupling only. We find the present choice quite convenient since, by duality arguments<sup>34</sup>, the critical point separating the large- $\Gamma$  quantum paramagnetic phase from the low- $\Gamma$  ferromagnetic region is known to be located at  $\Gamma_c = 1$ .

At the initial time  $t_{\text{in}} = -\infty$  the ground state of  $H(t_{\text{in}})$ , completely dominated by the transverse field term, is simply the state with all spins aligned along the  $+\hat{x}$  spin direction:  $|\Psi_{\text{in}}\rangle = \prod_i |\hat{x}\rangle_i = \prod_i [|\uparrow\rangle_i + |\downarrow\rangle_i]/\sqrt{2}$ . On the other side of the transition point  $\Gamma_c$ , the final Hamiltonian  $H(t_{\text{fin}}) = H_{cl}$  describes a *random ferromagnet* whose ground states, which we aim to reach by adiabatically switching off  $\Gamma(t)$ , are obviously the two trivial

states  $|\Psi_\uparrow\rangle = \prod_i |\uparrow\rangle_i$  and  $|\Psi_\downarrow\rangle = \prod_i |\downarrow\rangle_i$ : as an optimization problem,  $H_{\text{fin}}$  represents, therefore, a trivial problem.

Even if the ground states in the two limiting cases,  $\Gamma = \infty$  and  $\Gamma = 0$ , are very easy to find, when it comes to dynamics, the evolution dictated by  $H(t)$  is no longer a trivial problem. The instantaneous spectrum of the Hamiltonian  $H(t)$  is gapless in the thermodynamic limit<sup>34</sup>. This implies that, during the adiabatic evolution, defects in the form of domain walls between differently aligned ferromagnetic ground states, of the type

$$|\dots \uparrow\downarrow\downarrow\downarrow\downarrow\downarrow\uparrow\uparrow\uparrow\uparrow\uparrow\uparrow\downarrow\downarrow\downarrow\downarrow\dots\rangle$$

are formed, and reflected in a whole structure of closing gaps will appear in the instantaneous spectrum.

### A. Fermion representation and Bogoliubov-de Gennes equations

By means of the Jordan-Wigner transformation, the one-dimensional Ising model is reduced to a free fermion model. One first writes the spin operators in terms of hard-core bosons  $a_i$  and  $a_i^\dagger$  in a representation that maps the state  $|\sigma_i^z = +1\rangle \rightarrow |1\rangle_i = a_i^\dagger|0\rangle_i$  and  $|\sigma_i^z = -1\rangle \rightarrow |0\rangle_i$ , with the hard-core constraint  $(a_i^\dagger)^2|0\rangle_i = 0$ :  $\sigma_i^z = 2a_i^\dagger a_i - 1$ ,  $\sigma_i^x = a_i + a_i^\dagger$ , and  $\sigma_i^y = -i(a_i^\dagger - a_i)$ . The hard-core boson operators  $a_i$  are then re-expressed in terms of spinless fermions operators  $c_i$ :  $a_i = e^{i\pi \sum_{j<i} c_j^\dagger c_j} c_i$ . After a  $\pi/2$  rotation around the y-axis, which maps  $\sigma^x \rightarrow \sigma^z$  and  $\sigma^z \rightarrow -\sigma^x$ , the Hamiltonian in Eq.(1) can be rewritten in terms of fermion operators as

$$H = - \sum_i^{L-1} J_i \{c_i^\dagger c_{i+1}^\dagger + c_i^\dagger c_{i+1} + \text{H.c.}\} - 2\Gamma \sum_i^L h_i c_i^\dagger c_i, \quad (2)$$

where we have assumed open boundary conditions (OBC) for the spin-chain. For the case of periodic boundary conditions (PBC) on the spins,  $\sigma_{L+1} = \sigma_1$ , extra boundary terms appear in the fermionic Hamiltonian, of the form  $\Delta H_{\text{PBC}} = J_L(-1)^{N_F} \{c_L^\dagger c_1^\dagger + c_L^\dagger c_1 + \text{H.c.}\}$ , where  $N_F = \sum_i c_i^\dagger c_i$  is the total number of fermions. Notice that although  $N_F$  is not conserved by the Hamiltonian (2), the parity of  $N_F$  is conserved:  $(-1)^{N_F}$  is a constant of motion with value 1 or  $-1$ .

#### 1. Statics

The model in Eq. (2) can be diagonalized through a Bogoliubov rotation<sup>35,36</sup>, by introducing the new fermionic

operators  $\gamma_\mu$  and  $\gamma_\mu^\dagger$

$$\begin{aligned} \gamma_\mu &= \sum_{j=1}^L (u_{j\mu}^* c_j + v_{j\mu}^* c_j^\dagger) \\ c_i &= \sum_{\mu=1}^L (u_{i\mu} \gamma_\mu + v_{i\mu}^* \gamma_\mu^\dagger), \end{aligned} \quad (3)$$

where the  $L$ -dimensional vectors  $\mathbf{u}_\mu$  and  $\mathbf{v}_\mu$ , for  $\mu = 1, \dots, L$ , satisfy the Bogoliubov-de Gennes equations:

$$\begin{aligned} A \cdot \mathbf{u}_\mu + B \cdot \mathbf{v}_\mu &= \epsilon_\mu \mathbf{u}_\mu \\ -B \cdot \mathbf{u}_\mu - A \cdot \mathbf{v}_\mu &= \epsilon_\mu \mathbf{v}_\mu. \end{aligned} \quad (4)$$

Here  $A$  and  $B$  are real  $L \times L$  matrices whose non-zero elements are given by  $A_{i,i} = -\Gamma h_i$ ,  $A_{i,i+1} = A_{i+1,i} = -J_i/2$ ,  $B_{i,i+1} = -B_{i+1,i} = -J_i/2$ . (For the PBC spin-chain case, we have the additional matrix elements  $A_{L,1} = A_{1,L} = (J_L/2)(-1)^{N_F}$ , and  $B_{L,1} = -B_{1,L} = (J_L/2)(-1)^{N_F}$ ). While in the ordered case the solution of Eqs.(4) can be reduced, by switching to momentum-space, to independent  $2 \times 2$  problems, in the general disordered case one has to diagonalize the  $2L \times 2L$  problem numerically<sup>37,38</sup>.

The spectrum of Eqs. (4) turns out to be given by  $\pm\epsilon_\mu$ , with  $\epsilon_\mu \geq 0$ , and in terms of the new fermion operators,  $H$  becomes:

$$H = \sum_{\mu=1}^L (\epsilon_\mu \gamma_\mu^\dagger \gamma_\mu - \epsilon_\mu \gamma_\mu \gamma_\mu^\dagger) = \sum_{\mu=1}^L 2\epsilon_\mu (\gamma_\mu^\dagger \gamma_\mu - \frac{1}{2}). \quad (5)$$

The ground state of  $H$  is the Bogoliubov vacuum state  $|\Psi_0\rangle$  annihilated by all  $\gamma_\mu$  for  $\mu = 1 \dots L$ ,  $\gamma_\mu |\Psi_0\rangle = 0$ , with an energy  $E_0 = -\sum_{\mu=1}^L \epsilon_\mu$ .

#### 2. Dynamics

The Schrödinger dynamics associated to a time-dependent  $H(t)$  can be solved by a time-dependent Bogoliubov theory<sup>39</sup>. The basic fact that makes the solution possible even in the time-dependent case is that the Heisenberg's equations of motion for the operators  $c_{i,H}(t)$  are *linear*, because the Hamiltonian is quadratic:

$$i\hbar \frac{d}{dt} c_{i,H}(t) = 2 \sum_{j=1}^L \left[ A_{i,j}(t) c_{j,H}(t) + B_{i,j}(t) c_{j,H}^\dagger(t) \right]. \quad (6)$$

Here the matrices  $A$  and  $B$  have the same form given previously, except that now the time-dependence of  $\Gamma(t)$  is explicitly accounted for. If we denote by  $\gamma_{\mu,\text{in}}$  the Bogoliubov operators that diagonalize  $H(t_{\text{in}})$  at the initial time, and  $\mathbf{u}_\mu^{\text{in}}, \mathbf{v}_\mu^{\text{in}}$  the corresponding initial eigenvectors, it is simple to verify that the *Ansatz*

$$c_{i,H}(t) = \sum_{\mu=1}^L \left( u_{i\mu}(t) \gamma_{\mu,\text{in}} + v_{i\mu}^*(t) \gamma_{\mu,\text{in}}^\dagger \right), \quad (7)$$

does indeed solve the Heisenberg equations (6), provided the time-dependent coefficients  $u_{i\mu}(t)$  and  $v_{i\mu}(t)$ , satisfy the following system of first-order differential equations

$$\begin{aligned} i\frac{d}{dt}u_{i\mu}(t) &= \frac{2}{\hbar} \sum_{j=1}^L [A_{i,j}(t)u_{j\mu}(t) + B_{i,j}(t)v_{j\mu}(t)] \\ i\frac{d}{dt}v_{i\mu}(t) &= -\frac{2}{\hbar} \sum_{j=1}^L [A_{i,j}(t)v_{j\mu}(t) + B_{i,j}(t)u_{j\mu}(t)] \end{aligned} \quad (8)$$

with initial condition  $u_{i\mu}(t_{\text{in}}) = u_{i\mu}^{\text{in}}$ ,  $v_{i\mu}(t_{\text{in}}) = v_{i\mu}^{\text{in}}$ . Eqs. (8) are the natural time-dependent generalizations of the static Bogoliubov-de Gennes Eqs. (4), and, once again, they have to be solved numerically in the general disordered case.

### III. RESIDUAL ENERGY AND KINK DENSITY

How effectively the Schrödinger dynamics drives the system from the initial disordered quantum ground state  $|\Psi_{\text{in}}\rangle$  towards the classical ground state  $|\Psi_{\uparrow}\rangle = \prod_i |\uparrow\rangle_i$  (or the fully reversed one  $|\Psi_{\downarrow}\rangle = \prod_i |\downarrow\rangle_i$ )?

A way of quantifying the degree of adiabaticity of the evolution is given by the residual energy, defined as

$$E_{\text{res}} = E_{\text{fin}} - E_{\text{cl}} \quad (9)$$

where  $E_{\text{cl}} = -\sum_i J_i$  is the classical ground state energy of  $H(t_{\text{fin}}) = H_{\text{cl}}$ , and  $E_{\text{fin}} = \langle \Psi_{\text{fin}} | H_{\text{cl}} | \Psi_{\text{fin}} \rangle$  is the average classical energy of the final time-evolved state  $|\Psi_{\text{fin}}\rangle$ . Obviously,  $E_{\text{fin}}$ , and hence  $E_{\text{res}}$ , depends on the parameters specifying the evolution: the smaller and closer to  $E_{\text{cl}}$  the “slower” the evolution.

An alternative way of quantifying the degree of adiabaticity of the evolution, is given in terms of the density of kinks  $\rho_k$  in the final state, defined by

$$\rho_k = \frac{1}{L} \sum_i^{L-1} \langle \Psi(0) | \frac{1}{2} (1 - \sigma_i^z \sigma_{i+1}^z) | \Psi(0) \rangle \quad (10)$$

(for a PBC chain the sum goes up to  $L$ , instead of  $L-1$ ).

When no disorder is present the two quantities coincide, apart from trivial constants. In the disordered case, however, this is not the case. A defect will form with higher probability at a link where the corresponding exchange coupling  $J_i$  is small. Therefore the residual energy is not simply given by the kink density times the exchange coupling.

The calculation of quantities like  $E_{\text{fin}}$  or  $\rho_k$  is straightforward. Quite generally, given an operator  $\hat{O}[c_i, c_i^\dagger]$  expressed in terms of the  $c_i$ 's and  $c_i^\dagger$ 's, its expectation value over the final state  $|\Psi(t_{\text{fin}} = 0)\rangle$  can be expressed, switching from the Schrödinger to the Heisenberg picture, as  $\langle \Psi(0) | \hat{O}[c_i, c_i^\dagger] | \Psi(0) \rangle = \langle \Psi(t_{\text{in}}) | \hat{O}[c_{i,H}(0), c_{i,H}^\dagger(0)] | \Psi(t_{\text{in}}) \rangle$ . Next, one uses the expressions (7) for the  $c_{i,H}(0)$ 's and  $c_{i,H}^\dagger(0)$  in terms of

$\gamma_{\mu,\text{in}}, \gamma_{\mu,\text{in}}^\dagger, u_{i,\mu}(0)$ , and  $v_{i,\mu}(0)$ , and uses the fact that the  $\gamma_{\mu,\text{in}}$  annihilates by construction the initial state  $|\Psi(t_{\text{in}})\rangle$ .

By applying this procedure to the calculation of  $E_{\text{fin}}$  we get:

$$E_{\text{fin}} = \sum_{i,j} \left( A_{ij}(0) [v(0)v^\dagger(0) - u(0)u^\dagger(0)]_{ij} + B_{ij}(0) [v(0)u^\dagger(0) - u(0)v^\dagger(0)]_{ij} \right) \quad (11)$$

where  $u(0)$  and  $v(0)$  are  $L \times L$  matrices with elements  $u_{i,\mu}(0)$  and  $v_{i,\mu}(0)$ . Similarly, the density of defects  $\rho_k$  can also be expressed as:

$$\rho_k = \frac{1}{2L} \sum_i^{L-1} \left\{ 1 - ([v(0) - u(0)] [u^\dagger(0) + v^\dagger(0)])_{i,i+1} \right\} \quad (12)$$

### IV. RESULTS

Our results for the dynamics are obtained by integrating numerically the time-dependent Bogoliubov-de Gennes equations (8). As initial point of the evolution it is enough to consider  $t_{\text{in}} = -5\tau$ , taking  $\mathbf{u}_\mu^{\text{in}}$  and  $\mathbf{v}_\mu^{\text{in}}$  from the diagonalization of  $H(t_{\text{in}})$  according to Eq. (4): we checked that our results do not depend on the precise value of  $t_{\text{in}}$ , as long as it is not too small. We considered systems up to  $L = 512$  and annealing times up to  $\tau = 1000$ . Ensemble averages are calculated over a suitably large number of disorder realizations (of the order of 1000). The analysis of the instantaneous spectrum and its statistics has been obtained by solving the static Bogoliubov-de Gennes eigenvalue equations (4) for systems up to  $L = 512$ .

#### A. Landau-Zener transitions and disorder

In order to get an initial understanding on the mechanisms that lead to breaking of adiabaticity in the present system, it is instructive to consider in more detail the time-evolution of a single realization of the disorder. To be specific, Fig. (1) shows the time-evolution of the residual energy  $E_{\text{res}}(t) = \langle \Psi(t) | H(t) | \Psi(t) \rangle - E_{\text{gs}}(\Gamma(t))$ , where  $E_{\text{gs}}(\Gamma(t))$  is the instantaneous ground state energy corresponding to  $\Gamma(t)$ , for a single  $L = 64$  sample and for values of  $\tau$  up to 5000. We also plot the instantaneous spectral gaps of the problem (thick solid lines) obtained by diagonalizing the Hamiltonian for any given value of the parameter  $\Gamma$ . As mentioned previously, the dynamics conserves the fermion parity, so that only excitations in the same fermion parity sector are accessible. If we order the single-particle eigenvalues as  $\epsilon_1 \leq \epsilon_2 \leq \dots \leq \epsilon_L$ , then the lowest excited state accessible to the dynamics (i.e., conserving the fermionic parity) is associated with an excitation energy  $\Delta_1 = 2(\epsilon_1 + \epsilon_2)$ , rather than  $\Delta = 2\epsilon_1$ .

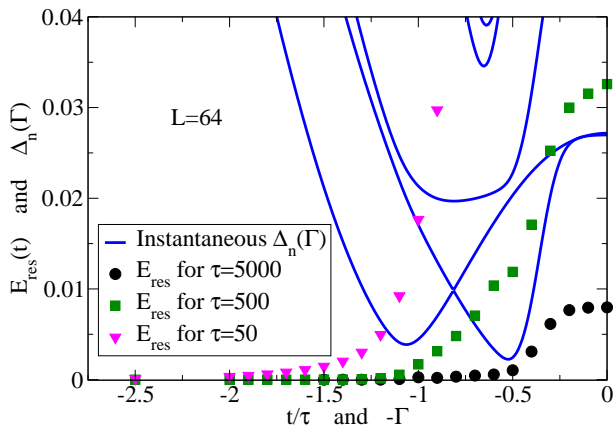


FIG. 1: (Color online) Residual energy  $E_{\text{res}}(t)$  versus  $t$  for a given instance with  $L = 64$  of the random Ising model with transverse field, at different values of  $\tau$ . The solid lines are the lowest-lying instantaneous spectral gaps  $\Delta_n$  as a function of  $\Gamma$ .

The next excited state is  $\Delta_2 = 2(\epsilon_1 + \epsilon_3)$ , and so on. These are the instantaneous gaps shown in Fig. (1).

An important feature which emerges from this example is that one cannot in general locate a single specific value of  $\Gamma$  where the minimum and most important gap is present. Certainly, typically the first occurrence of a small gap during the annealing trajectory is close to the critical point,  $\Gamma_c = 1$ . Usually, this critical-point gap is also the smallest one that the systems encounters during its evolution. However, it can happen, as Fig. (1) shows, that the system safely goes through the critical-point small gap (see  $\tau = 5000$  results) but then loses adiabaticity due to a comparable gap encountered later on (here at  $\Gamma \sim 0.5$ ). Once adiabaticity is lost, the system will generally miss to follow the first excited state either, getting more and more excited as time goes by.

It seems clear that the analysis of the adiabatic dynamics of a disordered Ising chain requires a knowledge of the statistics of these low-lying gaps in the spectrum (in the pertinent parity sector). We concentrate our attention on the region close to the critical point, where the smallest gaps are found, for large  $L$ .

We start asking how these smallest gaps are distributed, for different realizations of the disorder. Let us denote by  $P(\Delta_1, L)$  the distribution of gaps  $\Delta_1 = 2(\epsilon_1 + \epsilon_2)$  (the lowest one relevant for the dynamics) for a chain of length  $L$ , assumed to be normalized:  $\int_0^\infty d\Delta_1 P(\Delta_1, L) = 1$ . For the smallest gap  $\Delta = 2\epsilon_1$ , Young and Rieger<sup>37</sup> have shown that the correct scaling variable which makes the critical point distribution universal, for different  $L$ , is  $-\log(\Delta)/\sqrt{L}$ . By using a scaling variable of the same form,  $g = -\log(\Delta_1)/\sqrt{L}$ , we see that the gaps  $\Delta_1$  are also distributed in the same universal way, see Fig. (2). This implies that at the critical point,  $P_*(g) = \sqrt{L}e^{-g\sqrt{L}}P(e^{-g\sqrt{L}}; L)$  is, for large  $L$ , universal and normalized. As a consequence, gaps at the critical point have an extremely wide distribution,

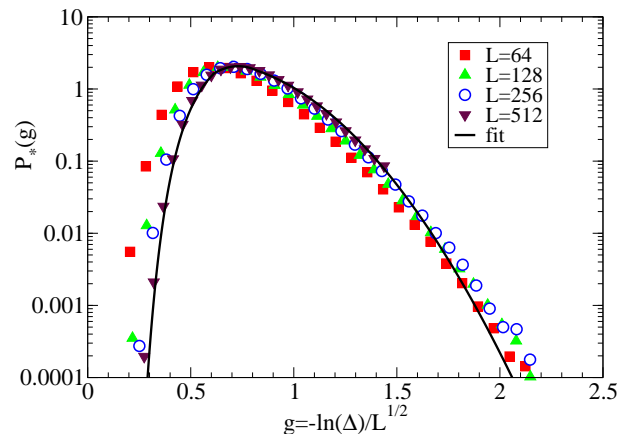


FIG. 2: (Color online) Distribution of  $\Delta_1 = 2(\epsilon_1 + \epsilon_2)$ , the smallest gap relevant for the dynamics, at the critical point  $\Gamma_c = 1$  for different system sizes, showing the collapse of the distributions  $P(\Delta_1, L)$  when the scaling variable  $g = -\log(\Delta_1)/\sqrt{L}$  is used. The resulting distribution is the  $P_*(g)$  discussed in the text.

for large  $L$ , with typical gaps which are exponentially small<sup>34,37,38</sup> in the system size:  $[\Delta_1]_{\text{typ}} \propto e^{-C\sqrt{L}}$ .

## B. Density of kinks

Given the wide distribution of the instantaneous gaps, it is important to understand how this reflects itself in the distribution of various observables. We first consider the behavior of the density of defects  $\rho_k$  defined in Eq.(10). The results for the probability distribution function of  $\rho_k$ ,  $P(\rho_k)$ , are presented in Fig. (3) for  $\tau = 10$  and  $\tau = 1000$ . The distribution  $P(\rho_k)$ , for given  $\tau$ , is found to be approximately log-normal:

$$P(\rho_k) = \frac{1}{\sqrt{2\pi}\sigma_L} \frac{1}{\rho_k} e^{-(\ln \rho_k - \overline{\ln \rho_k})^2 / 2\sigma_L^2},$$

with a standard deviation  $\sigma_L$  decreasing as  $1/\sqrt{L}$ . The data collapse of the results for different  $L$ , in terms of the variable  $(\ln \rho_k - \overline{\ln \rho_k})/\sigma_L$ , shown in the inset, qualifies the accuracy of this statement. This  $\sqrt{L}$ -reduction of the width of the log-normal distribution  $P(\rho_k)$  with increasing  $L$  is at variance with the result obtained for the distribution of the gaps at the critical point, whose width *increases* as  $\sqrt{L}$ : here, on the contrary, the correct scaling variable appears to be  $(\ln \rho_k - \overline{\ln \rho_k})\sqrt{L}$ , rather than  $(\ln \rho_k - \overline{\ln \rho_k})/\sqrt{L}$ . This width reduction, for increasing  $L$ , implies that the *average* density of defects  $[\rho_k]_{\text{av}}$  approaches the *typical* value  $[\rho_k]_{\text{typ}} = e^{[\ln \rho_k]_{\text{av}}}$  for large enough  $L$ , since  $[\rho_k]_{\text{av}} = e^{\overline{\ln \rho_k} + \sigma_L^2/2}$  implies that:

$$\frac{[\rho_k]_{\text{av}} - [\rho_k]_{\text{typ}}}{[\rho_k]_{\text{typ}}} = e^{\sigma_L^2/2} - 1 \sim \frac{1}{L}. \quad (13)$$

This fact is shown explicitly in Fig.(4) (top), where we see that large deviations between  $[\rho_k]_{\text{typ}} = e^{[\ln \rho_k]_{\text{av}}}$  and

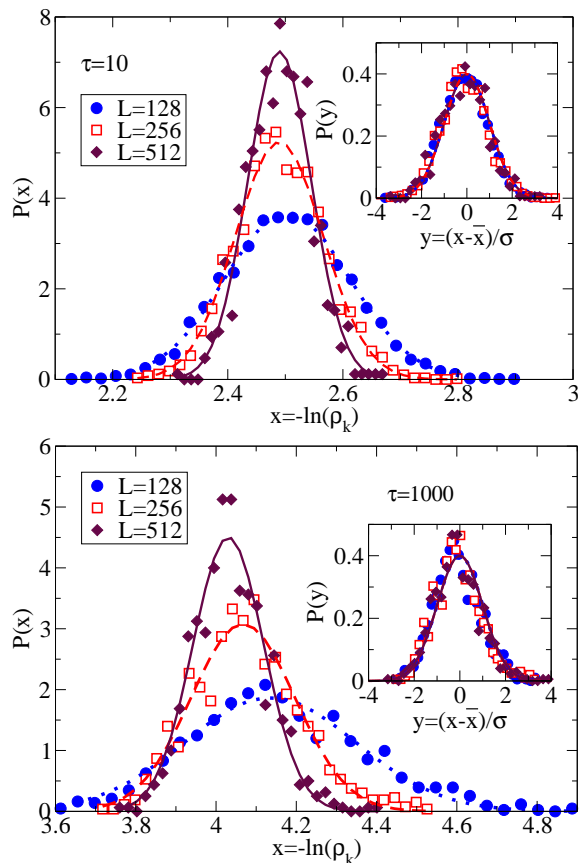


FIG. 3: (Color online) Probability distribution for the logarithm of the density of defects  $x = -\ln \rho_k$ , for two different annealing rates  $\tau$ . The distribution function is universal and log-normal with a variance  $\sigma_L$  which scales as  $1/\sqrt{L}$ . In the insets we show the data collapse of all the curves when plotted as a function of the reduced variable  $(x - \bar{x})/\sigma_L$ , where  $x = -\ln \rho_k$ .

$[\rho_k]_{\text{av}}$  are seen only for  $L \leq 64$ . For large systems,  $L \geq 128$ , the two quantities are essentially coincident, for all values of  $\tau$ . Despite the universal behavior of the distribution  $P(\rho_k)$  at all annealing rates, the behavior of  $[\rho_k]_{\text{av}}(\tau)$  changes drastically between short and long  $\tau$ 's<sup>33</sup>. Fig. (4)(bottom) focuses on the average kink density  $[\rho_k]_{\text{av}}$  for various  $L$ , as a function of  $\tau$ . The initial small- $\tau$  behavior of  $[\rho_k]_{\text{av}}(\tau)$ , indicated by the dashed line in Fig. (4), seems a power-law,  $[\rho_k]_{\text{av}}(\tau) \sim \tau^{-0.5}$ , i.e., exactly what one finds for the ordered Ising chain<sup>8</sup>, where the result is interpreted in terms of the the Kibble-Zurek mechanism. A possible explanation resides in the fact that our model presents a Griffiths phase extending for all  $\Gamma > \Gamma_c$ <sup>40</sup>. This phase is characterized by a gap  $\Delta \sim L^{-z}$ , where the dynamical exponent  $z(\Gamma)$  is a continuous function of the parameter  $\Gamma$ , diverging,  $z \rightarrow \infty$ , for  $\Gamma \rightarrow \Gamma_c$ , while saturating to a constant for large  $\Gamma$ . The second gap, which is relevant for our dynamical problem, shows a similar behavior,<sup>40</sup>  $\Delta_1 \sim L^{-z'}$ , with a dynamical exponent  $z'(\Gamma) = z(\Gamma)/2$ . For fast annealing rates,

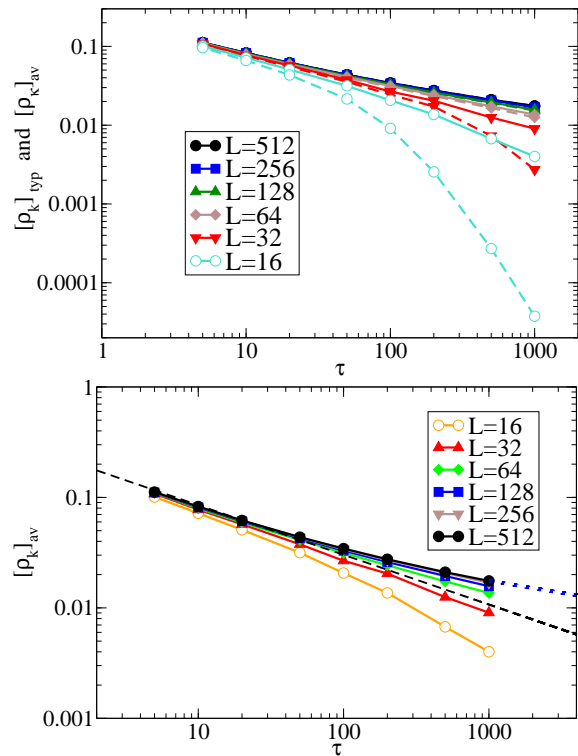


FIG. 4: (Color online) Top: Comparison between average  $[\rho_k]_{\text{av}}$  and typical  $[\rho_k]_{\text{typ}} = e^{[\ln \rho_k]_{\text{av}}}$  kink density for different system sizes on varying the annealing rate  $\tau$ . The same symbol is used for both cases. The typical value (dashed line) lies always below the average value (continuous line), but the difference between the two is negligible for  $L \geq 128$ . Bottom: Average kink density  $[\rho_k]_{\text{av}}$  as a function of the annealing rate  $\tau$  for chains of different lengths  $L = 16, 32, 64, 128, 256, 512$ . The data for  $[\rho_k]_{\text{av}}$  are the same appearing in the top part of the figure. The dashed line is a power-law describing the small- $\tau$  behavior,  $[\rho_k]_{\text{av}}(\tau) \sim \tau^{-0.5}$ . The solid thick line through the  $[\rho_k]_{\text{av}}$  data is a fit with a function  $A/\log^2(\gamma\tau)$ , described in the text. The averages are calculated over 1000 different realizations of disorder.

the system loses adiabaticity before reaching the critical point, well inside the  $\Gamma > \Gamma_c$  Griffiths phase. As in the ordered case, the gaps exhibited by such a phase would induce a defect density decreasing as a power-law of the annealing time  $\tau$ , with the crucial difference that the power-law exponent is not constant here, due to the  $\Gamma$ -dependence of  $z'$ . One should expect, presumably, a gradual crossover with a power-law exponent which becomes smaller and smaller, connecting in a gentle way with the large  $\tau$  behavior of  $[\rho_k]_{\text{av}}$ , which shows marked deviations from a power-law behavior. Dziarmaga, based on scaling arguments<sup>33</sup> showed that at large  $\tau$  the density of kinks should decrease as the inverse square of the logarithm of  $\tau$ . Our data for the largest systems agree very well with this prediction, as the best-fit (solid line in Fig. (4)) shows.

A bound to  $[\rho_k]_{\text{av}}(\tau)$  can also be constructed by a Landau-Zener argument — complemented by a knowl-

edge of the distribution of the first gap  $P(\Delta_1, L)$  —, in a similar fashion to that presented by Zurek *et al.*<sup>8</sup> for the ordered Ising case. The derivation starts by considering the probability  $P_{\text{ex}}(\tau, L)$  of loosing adiabaticity for a system of size  $L$ , when turning off  $\Gamma$  with an annealing rate  $\tau^{-1}$ . Evidently,  $P_{\text{ex}}(\tau, L) \geq P_{\text{ex}}^{\text{cr.point}}(\tau, L)$ , where we have denoted by  $P_{\text{ex}}^{\text{cr.point}}(\tau, L)$  the probability of getting excited by Landau-Zener events *at the critical point* (indeed, we have seen that there is a chance of getting excited also by gaps well below the critical point).  $P_{\text{ex}}^{\text{cr.point}}(\tau, L)$ , in turn, can be constructed by knowing the distribution of the gaps  $\Delta_1$  at the critical point, and the simple two-level Landau-Zener formula  $P_{\text{ex}}^{\text{LZ}} = e^{-\pi\Delta_1^2\tau/(4\hbar\alpha)}$  ( $\alpha$  being the slope of the two approaching eigenvalues). Lumping all constants together,  $\gamma = \pi/(4\hbar\alpha)$ , we write  $P_{\text{ex}}^{\text{LZ}} = e^{-\gamma\tau\Delta_1^2}$  and assume that the distribution of  $\gamma \propto \alpha^{-1}$  is not important in our estimate, while that of  $\Delta_1$  is, so that:

$$\begin{aligned} P_{\text{ex}}^{\text{cr.point}}(\tau, L) &= \int_0^\infty d\Delta_1 P(\Delta_1, L) e^{-\gamma\tau\Delta_1^2} \\ &= \int_{-\infty}^\infty dg P_*(g) e^{-\gamma\tau e^{-2\sqrt{L}g}}, \end{aligned} \quad (14)$$

where the second equality follows from switching to the scaling variable  $g = -\log(\Delta_1)/\sqrt{L}$ . Obviously, for  $\tau = 0$  we correctly have  $P_{\text{ex}}^{\text{cr.point}}(\tau = 0, L) = \int_{-\infty}^\infty dg P_*(g) = 1$ , from the normalization condition. When  $\tau$  is finite, the LZ factor  $e^{-\gamma\tau e^{-2\sqrt{L}g}}$  provides a lower cut-off in the integral at a characteristic  $g_c = \log(\gamma\tau)/(2\sqrt{L})$ , and this cut-off is sharper and sharper as  $L$  increases: one can verify that, for large  $L$ ,  $e^{-\gamma\tau e^{-2\sqrt{L}g}} \approx \theta(g - g_c)$ . As a consequence, for large enough  $L$  we can rewrite:

$$P_{\text{ex}}^{\text{cr.point}}(\tau, L) \approx \Pi(g_c) \equiv \int_{g_c}^\infty dg P_*(g), \quad (15)$$

i.e.,  $P_{\text{ex}}^{\text{cr.point}}(\tau, L)$  turns out to be a universal function of the scaling variable  $g_c = \log(\gamma\tau)/(2\sqrt{L})$ , for  $L$  large. This universal function  $\Pi(g_c)$  is shown in Fig.(5), where we see that data for  $L \geq 512$  collapse into a single curve. The density of kinks for large  $\tau$ , and large enough  $L$ , can be obtained by evaluating the typical length  $\tilde{L}_\epsilon(\tau)$  of a defect-free region upon annealing,  $\epsilon$  being a small quantity of our choice, denoting the probability of getting excited. Since  $P_{\text{ex}}^{\text{cr.point}}(\tau, L) \approx \Pi(g_c)$  is a *lower bound* for  $P_{\text{ex}}(\tau, L)$ , we have that

$$\tilde{L}_\epsilon(\tau) \leq \frac{\log^2(\gamma\tau)}{[\Pi^{-1}(\epsilon)]^2}, \quad (16)$$

where  $\Pi^{-1}$  denotes the inverse function of  $\Pi$ . If we now identify the inverse of the defect-free region length,  $\tilde{L}_\epsilon^{-1}(\tau)$ , with the density of kinks  $\rho_k(\tau)$ , we get the following lower bound for the latter:

$$\rho_k(\tau) \sim \frac{1}{\tilde{L}_\epsilon(\tau)} \geq \frac{[\Pi^{-1}(\epsilon)]^2}{\log^2(\gamma\tau)}. \quad (17)$$

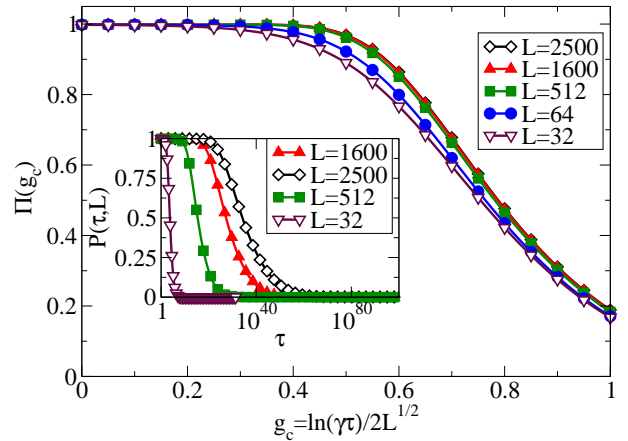


FIG. 5: (Color online) Approach to the universal function  $\Pi(g_c)$  for increasing chain lengths  $L$ , see text. All data from  $L \geq 512$  collapse well into a single curve. Inset:  $P_{\text{ex}}^{\text{cr.point}}(\tau, L)$  obtained from the integral in Eq. (14) versus  $\tau$  for different values of  $L$ .

On the basis of this argument, we conclude that the density of kinks cannot decrease faster than  $1/\log^2(\gamma\tau)$  for large  $\tau$ , which agrees with the argument discussed by Dziarmaga<sup>33</sup>.

### C. Residual energy

In the ordered case the residual energy per spin is simply proportional to the kink-density,  $E_{\text{res}}/L = 2J\rho_k$ , while here, evidently, kinks sitting at small  $J_i$ 's are favored, on average, by the adiabatic evolution process. It is therefore of importance to analyze the scaling of the residual energy that, as we will show, differs quantitatively from that of the kink density. Since kinks will be formed on the weak links, one expects on general grounds that the residual energy would decay faster than the kink-density for large  $\tau$ 's.

As in the case of the kink density, we first analyze the probability distribution for the residual energy per site, which we present in Fig.(6). Once again the residual energies are approximately log-normal distributed and can be reduced to a universal form (see the insets) when properly rescaled, i.e., in terms of the variable  $(\ln(E_{\text{res}}/L) - \ln(\overline{E_{\text{res}}/L}))\sqrt{L}$ .

The average residual energy per site  $[E_{\text{res}}/L]_{\text{av}}$  as a function of the annealing time  $\tau$  shows a crossover from a power-law decay, approximately  $\tau^{-1}$  for fast quenches, to a much slower decay (see below) for slow evolutions. It is interesting to note that although for fast quenches the disorder is considered to play a minor role, nevertheless the exponent of the decay of the residual energy differs from that of the kink density. The analysis of the regimes of large  $\tau$ 's is more delicate. The LZ argument given above tells us nothing about the behavior of the residual energy for large  $\tau$ . We then proceed as follows. Assuming

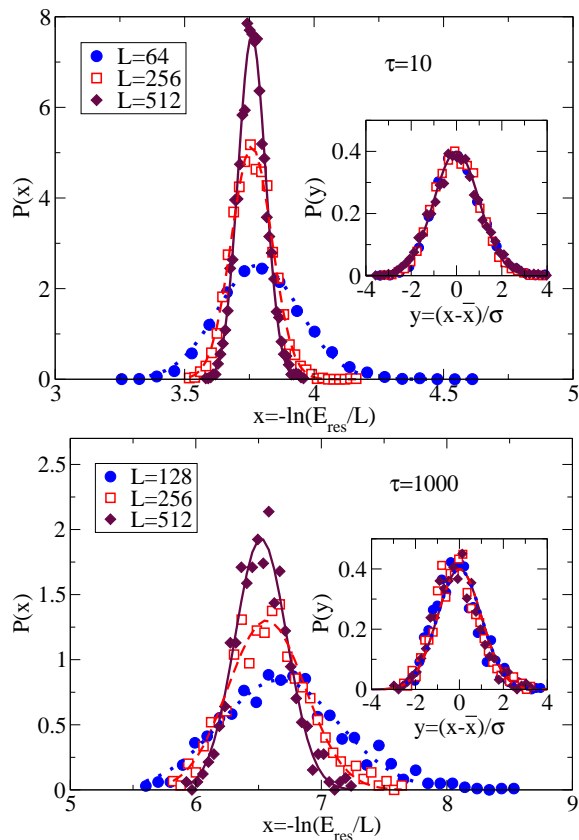


FIG. 6: (Color online) Probability distribution for the residual energy per site at two different annealing rates  $\tau^{-1}$ . The distribution function is universal and log-normal with a variance which scales as  $1/\sqrt{L}$ . In the insets we show the data collapse.

for the residual energy a logarithmic behavior similar to that found for  $\rho_k$

$$\left[ \frac{E_{\text{res}}}{L} \right]_{\text{av}} \sim \frac{1}{\log^\zeta(\gamma\tau)}, \quad (18)$$

we can determine  $\zeta$  from the data of Fig. (7)(Top) by plotting the ratio of  $[\rho_k]_{\text{av}}^\alpha$  and  $[E_{\text{res}}/L]_{\text{av}}$  versus  $\tau$  for several values of  $\alpha$ , as done in Fig. (7)(Bottom). If  $[\rho_k]_{\text{av}} \sim \log^{-2}(\gamma\tau)$ , then the value of  $\alpha$  which makes this ratio constant is:

$$\frac{[\rho_k]_{\text{av}}^\alpha}{[E_{\text{res}}/L]_{\text{av}}} \propto \log^{\zeta-2\alpha}(\gamma\tau) \sim \text{const.} \iff \alpha = \zeta/2. \quad (19)$$

Numerically, see Fig. (7), we find  $\alpha \approx 1.7 \pm 0.1$ , which implies  $\zeta \approx 3.4 \pm 0.2$ .

## V. DISCUSSION AND CONCLUSIONS

In this paper we have studied the adiabatic quantum dynamics of a one-dimensional disordered Ising model

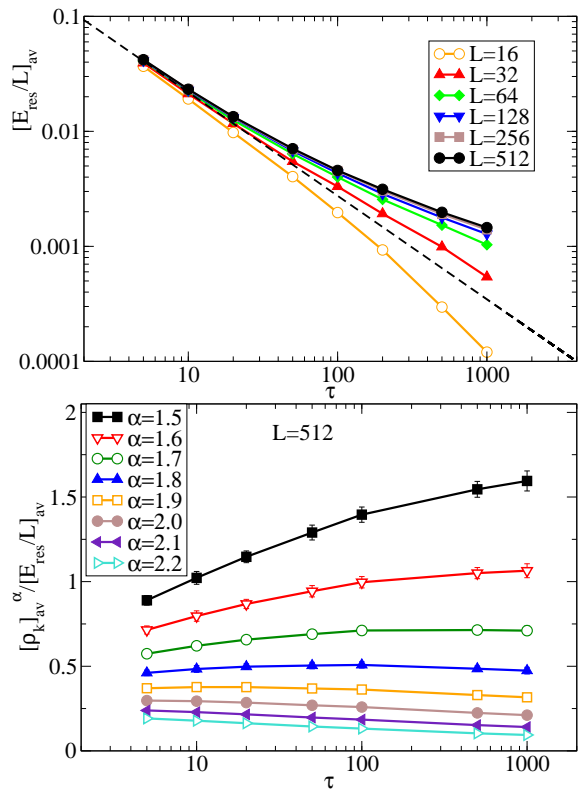


FIG. 7: (Color online) Top: Average residual energy per site  $[E_{\text{res}}/L]_{\text{av}}$  as functions of the annealing rate  $\tau$  for chains of different lengths  $L = 16, 32, 64, 128, 256, 512$ . The dashed line is the power-law describing the small- $\tau$  behavior,  $[E_{\text{res}}/L]_{\text{av}}(\tau) \sim \tau^{-1}$ . Averages are calculated over 1000 realizations of disorder. Bottom: The ratio of the density of kinks and the residual energy versus  $\tau$ , used to extract the power of the log-dependence of  $E_{\text{res}}$ .

across its quantum critical point. Our main results can be summarized in the dependence of the average kink density (see however<sup>33</sup>) and residual energies as a function of the annealing rate

$$\begin{aligned} [\rho_k]_{\text{av}} &\sim \tau^{-0.5} && \text{fast quenches} \\ [\rho_k]_{\text{av}} &\sim (\log \tau)^{-2} && \text{large } \tau, \end{aligned}$$

$$\begin{aligned} [E_{\text{res}}/L]_{\text{av}} &\sim \tau^{-1} && \text{fast quenches} \\ [E_{\text{res}}/L]_{\text{av}} &\sim (\log \tau)^{-\zeta} && \text{large } \tau, \text{ with } \zeta \sim 3.4. \end{aligned}$$

Although the dynamics is dominated by a very wide distribution of gaps at the critical point,  $P_*(-\ln(\Delta_1)/\sqrt{L})$  (see Fig. (2)), we find that the distribution for both these quantities are log-normal but with a variance that decrease, like  $1/\sqrt{L}$ , for increasing chain length  $L$ : typical and average values, therefore, coincide for large  $L$ . The wide distribution of gaps, on the other hand, with its characteristic  $\ln(\Delta_1)/\sqrt{L}$  scaling, is responsible, within a Landau-Zener theory, for the extremely slow decay of the average density of kinks,  $[\rho_k]_{\text{av}} \sim 1/(\ln \tau)^2$ . This discussion applies only for reasonably large sizes  $L$ . If  $L$  is

small, the minimum gap  $\Delta_1$  of a given instance can be sufficiently large that the adiabatic regime, predicted to occur beyond a characteristic  $\tau_c \propto \Delta_1^{-2}$ , is actually seen: a fast decay of  $\rho_k$  and  $E_{\text{res}}/L$  is expected<sup>41</sup> for  $\tau > \tau_c$ , in such a case.

It is interesting to compare these results with those of a classical thermal annealing, where, according to Huse and Fisher<sup>42</sup>, the residual energy also shows a logarithmic behavior

$$E_{\text{res}}^{\text{CA}}(\tau)/L \sim (\log \tau)^{-\zeta_{\text{CA}}} \quad \zeta_{\text{CA}} \leq 2,$$

but with an exponent  $\zeta_{\text{CA}}$  which is bound by  $\zeta_{\text{CA}} \leq 2$ .

If we look at this problem from the perspective of optimization algorithms, it seems that quantum annealing (QA) gives a quantitative improvement over classical annealing for the present system, as is indeed found in other cases<sup>3,5,43,44,45,46,47,48,49</sup>, but not always (Boolean Satisfiability problems seem to be a test case where QA performs worse than classical annealing, see Ref. 50).

In this respect, however, several important issues remain to be clarified. First of all, AQC-QA has a large freedom in its construction: the choice of the possible source of quantum fluctuations<sup>51</sup> — generally speaking, one can take  $H(t) = H_{\text{fin}} + \sum_{\lambda} \Gamma_{\lambda}(t) H_{\lambda}$  —, and the time-dependence of the various  $\Gamma_{\lambda}(t)$ , which need not be linear in time<sup>12,13</sup>. Regarding the time dependence of the couplings, we simply note that an optimal choice of the “speed”  $\Gamma(t)$  with which the critical point is crossed can provide an improvement in the exponents<sup>13</sup>, but definitely not change a logarithm into a power-law. Regarding the possibility of adding extra kinetic terms to  $H(t)$ , it is clear that terms like  $-\Gamma_{xy}(t) \sum_i J_i \sigma_i^x \sigma_{i+1}^y$  (XY-anisotropy) or similar short range interactions will not

change the universality class of the infinite randomness quantum critical point of the present model<sup>34</sup>. Hence, a logarithmically-slow AQC-QA is expected also in more general circumstances, for the present one-dimensional model. We expect this to be a genuine consequence of the randomness present in the problem at hand, which makes the adiabatic quantum dynamics intrinsically slow and ineffective in reaching the simple classical ferromagnetic ground states<sup>52,53</sup>.

This is perhaps to be expected in view of the results of Vidal<sup>54</sup>, who showed that problems where the entanglement entropy of a block is bound, can be computed classically with a comparable efficiency. Generically, in disordered one-dimensional system the entanglement entropy grows at most logarithmically with the system size at a critical point<sup>55,56,57</sup>, at this is not enough to substantially change the relative efficiency of quantum versus classical algorithms.

Therefore, the route to investigate seems to be following: search for models in more than one-dimension, where the entropy of entanglement grows stronger, which, at the same time, have “gentle” enough critical point gap distributions.

Acknowledgments — We are grateful to E. Tosatti, A. Scardicchio, S. Suzuki, H. Nishimori, A. Ekert, S. Masida, V. Giovannetti, S. Montangero, J.R. Laguna, G. De Chiara, and W.H. Zurek for discussions. This research was partially supported by MIUR-PRIN and EC-Eurosqip. The present work has been performed within the “Quantum Information” research program of the *Centro di Ricerca Matematica “Ennio De Giorgi”* at the Scuola Normale Superiore in Pisa.

- 
- <sup>1</sup> E. Farhi, J. Goldstone, S. Gutmann, J. Lapan, A. Lundgren, and D. Preda, *Science* **292**, 472 (2001).
- <sup>2</sup> A. B. Finnila, M. A. Gomez, C. Sebenik, C. Stenson, and J. D. Doll, *Chem. Phys. Lett.* **219**, 343 (1994).
- <sup>3</sup> T. Kadowaki and H. Nishimori, *Phys. Rev. E* **58**, 5355 (1998).
- <sup>4</sup> J. Brooke, D. Bitko, T. F. Rosenbaum, and G. Aeppli, *Science* **284**, 779 (1999).
- <sup>5</sup> G. E. Santoro, R. Martoňák, E. Tosatti, and R. Car, *Science* **295**, 2427 (2002).
- <sup>6</sup> A. Das and B. K. Chakrabarti, *Quantum Annealing and Related Optimization Methods*, Lecture Notes in Physics (Springer-Verlag, 2005).
- <sup>7</sup> G. E. Santoro and E. Tosatti, *J. Phys. A: Math. Gen.* **39**, R393 (2006).
- <sup>8</sup> W. H. Zurek, U. Dorner, and P. Zoller, *Phys. Rev. Lett.* **95**, 105701 (2005).
- <sup>9</sup> M. Nielsen and I. L. Chuang, *Quantum Computation and Quantum Information* (Cambridge University Press, 2000).
- <sup>10</sup> D. Aharonov, W. van Dam, J. Kempe, Z. Landau, S. Lloyd, and O. Regev, in *Proceedings of the 45th Annual IEEE Symposium of Foundations of Computer Science (FOCS'04)* (2004), p. 42.
- <sup>11</sup> D. Aharonov, W. van Dam, J. Kempe, Z. Landau, S. Lloyd, and O. Regev, *quant-ph/0405098*.
- <sup>12</sup> In order to optimize the adiabatic algorithm one should also find the optimal time dependence of the coupling constant  $\Gamma(t)$ , see Ref. 13.
- <sup>13</sup> J. Roland and N. J. Cerf, *Phys. Rev. A* **65**, 042308 (2002).
- <sup>14</sup> T. W. B. Kibble, *Phys. Rep.* **67**, 183 (1980).
- <sup>15</sup> W. H. Zurek, *Phys. Rep.* **276**, 177 (1996).
- <sup>16</sup> C. Bauerle, Y. M. Bunkov, S. N. Fisher, H. Godfrin, and G. R. Pickett, *Nature* **382**, 332 (1996).
- <sup>17</sup> V. M. H. Ruutu, V. B. Eltsov, A. J. Gill, T. W. B. Kibble, M. Krusius, Y. G. Makhlin, B. Placais, G. E. Volovik, and W. Xu, *Nature* **382**, 334 (1996).
- <sup>18</sup> A. Polkovnikov, *Phys. Rev. B* **72**, 161201(R) (2005).
- <sup>19</sup> For a general approach see also Ref. 20.
- <sup>20</sup> A. Polkovnikov and V. Gritsev (2007), *arXiv:0706.0212*.
- <sup>21</sup> J. Dziarmaga, *Phys. Rev. Lett.* **95**, 245701 (2005).
- <sup>22</sup> P. Pfeuty, *Ann. Phys. (N.Y.)* **57**, 79 (1970).
- <sup>23</sup> B. Damski, *Phys. Rev. Lett.* **95**, 035701 (2005).
- <sup>24</sup> B. Damski and W. H. Zurek, *Phys. Rev. A* **73**, 063405 (2006).
- <sup>25</sup> R. W. Cherng and L. Levitov, *Phys. Rev. A* **73**, 043614

- (2006).
- <sup>26</sup> A. Fubini, A. Osterloh, and G. Falci, to appear in *New. J. Phys.*, cond-mat/0702014.
- <sup>27</sup> R. Schützhold, M. Uhlmann, Y. Xu, and U. R. Fischer, *Phys. Rev. Lett.* **97**, 200601 (2006).
- <sup>28</sup> F. M. Cucchietti, B. Damski, J. Dziarmaga, and W. H. Zurek, *Phys. Rev. A* **75**, 023603 (2007).
- <sup>29</sup> J. Latorre and R. Orus, *Phys. Rev. A* **69**, 062302 (2004).
- <sup>30</sup> L. Cincio, J. Dziarmaga, M. M. Rams, and W. H. Zurek, *Phys. Rev. A* **75**, 052321 (2007).
- <sup>31</sup> J. J. Hopfield and D. W. Tank, *Science* **233**, 625 (1986).
- <sup>32</sup> M. Mézard, G. Parisi, and R. Zecchina, *Science* **297**, 812 (2002).
- <sup>33</sup> J. Dziarmaga, *Phys. Rev. B* **74**, 064416 (2006).
- <sup>34</sup> D. S. Fisher, *Phys. Rev. B* **51**, 6411 (1995).
- <sup>35</sup> E. Lieb, T. Schultz, and D. Mattis, *Ann. Phys. (N.Y.)* **16**, 407 (1961).
- <sup>36</sup> A. Young, *Phys. Rev. B* **56**, 11691 (1997).
- <sup>37</sup> A. P. Young and H. Rieger, *Phys. Rev. B* **53**, 8486 (1996).
- <sup>38</sup> D. S. Fisher and A. P. Young, *Phys. Rev. B* **58**, 9131 (1998).
- <sup>39</sup> E. Barouch, B. M. McCoy, and M. Dresden, *Phys. Rev. A* **2**, 1075 (1970).
- <sup>40</sup> F. Igloi, R. Juhasz, and H. Rieger, *Phys. Rev. B* **59**, 11308 (1999).
- <sup>41</sup> S. Suzuki and M. Okada, *J. Phys. Soc. Jpn.* **74**, 1649 (2005).
- <sup>42</sup> D. A. Huse and D. S. Fisher, *Phys. Rev. Lett.* **57**, 2203 (1986).
- <sup>43</sup> Y. H. Lee and B. J. Berne, *J. Phys. Chem. A* **104**, 86 (2000).
- <sup>44</sup> Y. H. Lee and B. J. Berne, *J. Phys. Chem. A* **105**, 459 (2001).
- <sup>45</sup> R. Martoňák, G. E. Santoro, and E. Tosatti, *Phys. Rev. B* **66**, 094203 (2002).
- <sup>46</sup> P. Liu and B. J. Berne, *J. Chem. Phys.* **118**, 2999 (2003).
- <sup>47</sup> R. Martoňák, G. E. Santoro, and E. Tosatti, *Phys. Rev. E* **70**, 057701 (2004).
- <sup>48</sup> L. Stella, G. E. Santoro, and E. Tosatti, *Phys. Rev. B* **72**, 014303 (2005).
- <sup>49</sup> L. Stella, G. E. Santoro, and E. Tosatti, *Phys. Rev. B* **73**, 144302 (2006), cond-mat/0512064.
- <sup>50</sup> D. A. Battaglia, G. E. Santoro, and E. Tosatti, *Phys. Rev. E* **71**, 066707 (2005).
- <sup>51</sup> S. Suzuki, H. Nishimori, and M. Suzuki, *Phys. Rev. E* **75**, 051112 (2007).
- <sup>52</sup> We mention, however, that for finite-size Ising systems, convergence bound have been proved for AQC-QA in terms of power-law annealing schedules, see Ref. 53.
- <sup>53</sup> S. Morita and H. Nishimori, *J. Phys. A* **39**, 13903 (2006).
- <sup>54</sup> G. Vidal, *Phys. Rev. Lett.* **91**, 147902 (2003).
- <sup>55</sup> G. Refael and J. Moore, *Phys. Rev. Lett.* **93**, 260602 (2004).
- <sup>56</sup> N. Laflorencie, *Phys. Rev. B* **72**, 140408(R) (2005).
- <sup>57</sup> G. De Chiara, S. Montanegro, P. Calabrese, and R. Fazio, *J. Stat. Mech.* p. 0602P001 (2006).